

Quark anomalous magnetic moment in an extreme magnetic background from perturbative QCD

Eduardo S. Fraga^{⊗,1,*} Leticia F. Palhares^{⊗,2,†} and Cristian Villavicencio^{⊗,3,‡}

¹*Instituto de Física, Universidade Federal do Rio de Janeiro,
Caixa Postal 68528, 21941-972, Rio de Janeiro, RJ, Brazil*

²*Departamento de Física Teórica, Universidade do Estado do Rio de Janeiro,
Rua São Francisco Xavier 524, 20550-013, Rio de Janeiro, Brazil*

³*Centro de Ciencias Exactas and Departamento de Ciencias Básicas, Facultad de Ciencias,
Universidad del Bío-Bío, Casilla 447, Chillán, Chile*



(Received 21 March 2024; accepted 23 May 2024; published 21 June 2024)

We compute the one-loop QCD correction to the photon-quark-antiquark vertex in an extremely strong magnetic background, i.e., one in which \sqrt{eB} is much larger than all other mass scales. We resort to the lowest-Landau level approximation, and consider on-shell fermions. We find that the total magnetic moment is such that the anomalous magnetic moment contributes to the electric part $\sim iE_3\sigma_3$, the other contributions to $\mathbf{B} \cdot \boldsymbol{\sigma}$ and $i\mathbf{E} \cdot \boldsymbol{\sigma}_\perp$ being completely suppressed. We show results for the anomalous magnetic moment of quarks up and down, scaled by their values in the vacuum, as a function of the external magnetic field, considering dressed gluons and a renormalization scale $\mu_{\overline{\text{MS}}} = \sqrt{|eB|}$.

DOI: 10.1103/PhysRevD.109.116018

I. INTRODUCTION

The original one-loop calculation of the anomalous magnetic moment [1], together with the spectacular agreement with experimental data that followed refined higher-order perturbative calculations (see Ref. [2] for a review), represents a major landmark of theoretical physics.

The one-loop correction to the anomalous magnetic moment (AMM) of a fermion that moves in the presence of an external magnetic background will, however, deviate from the original prediction by Schwinger of $\alpha/2\pi$ [1,3], where $\alpha \approx 1/137$ is the QED fine-structure constant. This was already known by Schwinger, since what is currently known as the *Schwinger phase* appears in each fermion propagator [4]. The functional dependence of this correction on the magnitude of the external magnetic field has first been addressed almost half a century ago [5,6].

Motivated by the ultrastrong magnetic fields that can be achieved in current experiments at the Large Hadron Collider (LHC), we compute the one-loop perturbative QCD correction to the photon-quark-antiquark vertex in an

extremely strong magnetic background, i.e., one in which \sqrt{eB} is much larger than all other mass scales. Here e is the fundamental electric charge and B is the magnetic field strength. For such high fields, we can resort to the lowest-Landau level (LLL) approximation, and consider on-shell fermions.

The AMM of quarks in the presence of an external magnetic field can be related to the phenomenon of magnetic catalysis [7–9] and, in the presence of a hot plasma, might play a role in the so-called chiral magnetic effect [10]. The ultrahigh magnetic fields that can be produced in high-energy heavy ion collisions [11–13] bring the question of whether the AMM might prove to be experimentally relevant in this physical setting. Therefore, effects from the AMM have been under investigation in quark and hadronic matter for over two decades [14–32].

Usually, estimates of magnetic corrections to the fermion AMM are based on the Schwinger ansatz [4], which relates the AMM with the tensor spinor structure of the self-energy. On the other hand, not much has been done in obtaining the AMM from radiative corrections to the fermion-photon coupling. The AMM has been calculated from the fermion-photon vertex, including magnetic field corrections, using the Schwinger proper-time method for low magnetic fields [33].

In the paper at hand, conversely, we explore the magnetic effects on the *quark* AMM in the presence of a *very intense* magnetic background. We find that the total magnetic moment is such that the AMM in the presence of a very strong magnetic background contributes to the electric part

*fraga@if.ufrj.br

†leticia.palhares@uerj.br

‡cvillavicencio@ubiobio.cl

Published by the American Physical Society under the terms of the [Creative Commons Attribution 4.0 International license](https://creativecommons.org/licenses/by/4.0/). Further distribution of this work must maintain attribution to the author(s) and the published article's title, journal citation, and DOI. Funded by SCOAP³.

$\sim iE_3\sigma_3$, which should not be confused with an anomalous electric dipole moment [34]. The other AMM contributions to $\mathbf{B} \cdot \boldsymbol{\sigma}$ and $i\mathbf{E} \cdot \boldsymbol{\sigma}_\perp$ are completely suppressed.

We also show results for the anomalous magnetic moment of quarks up and down, scaled by their values in the vacuum, as a function of the external magnetic field, considering dressed gluons and a renormalization scale $\mu_{\overline{\text{MS}}} = \sqrt{|eB|}$. We consider two scenarios: one with a constant gluon mass, $m_g = 0.3$ GeV, and one with the gluon mass extracted from the one-loop correction to its polarization tensor in the presence of a large external magnetic field.

The paper is organized as follows. In Sec. II we present the general formalism. First, we outline the computation of the anomalous correction in QED. Then, we compute the AMM of QCD in a strong magnetic background, with special emphasis on the QCD correction to the vertex triangular diagram that contributes to the structure function F_2 . In Sec. III we present and discuss our results for the QCD correction to the AMM as a function of the magnetic field in a few phenomenological scenarios. Finally, Sec. IV contains our summary and outlook.

II. ANOMALOUS MAGNETIC MOMENT: FORMALISM

A. Outline of AMM in one-loop QED

In order to set the notation and define the main physical quantities, we start with a brief discussion of well-known textbook results for the anomalous magnetic moment in QED (see, e.g., Ref. [34]).

The Dirac equation

$$[i\mathcal{D} - m]\psi = 0 \quad (1)$$

provides, at tree level, the fermion-antifermion-photon vertex $e_q \bar{u}(p') \gamma^\mu u(p)$, where m is the spinor mass, e_q its electric charge ($e_q = -e$ for the electron), and $D_\mu = \partial_\mu + ie_q A_\mu$ the covariant derivative. Here, we use the Weyl representation for the Dirac gamma matrices in Minkowski space. The equation of motion naturally exhibits the AMM when written in quadratic form, so that charged spinors in an electromagnetic field $F_{\mu\nu}$ satisfy

$$\left[D^2 + m^2 - \frac{e_q}{2} F_{\mu\nu} \sigma^{\mu\nu} \right] \psi = 0, \quad (2)$$

where $[D_\mu, D_\nu] = -ie_q F_{\mu\nu}$, and $\sigma^{\mu\nu} = \frac{i}{2} [\gamma^\mu, \gamma^\nu]$. One-loop corrections bring about other structures, with terms proportional to $(p' + p)$ and $(p' - p)$. In this case, one can resort to the Gordon identity

$$\bar{u}(p')(p'^\mu + p^\mu)u(p) = \bar{u}(p')[2m\gamma^\mu - i\sigma^{\mu\nu}(p'_\nu - p_\nu)]u(p), \quad (3)$$

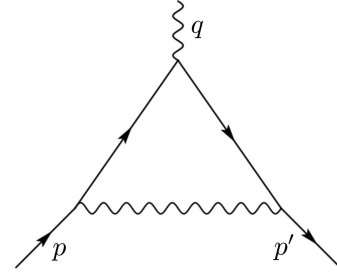


FIG. 1. Vertex triangular diagram from QED that contributes to F_2 .

where the fermions are on shell. The photon momentum $q = p' - p$ can be recognized in the previous equation, so the contribution to the fermion-photon vertex γ_μ is interpreted as a correction to the fermion charge, while the term $\sigma_{\mu\nu} q^\nu$ is identified with the AMM.

At any loop order, the vertex is constrained by Lorentz symmetry, the Dirac equation for spinors, $k_i u(k_i) = m u(k_i)$, the Ward identity, and the Gordon identity. So, one can write it in the following standard form:

$$\mathcal{M}^\mu = e_q \bar{u}(p') \left[F_1 \left(\frac{q^2}{m^2} \right) \gamma^\mu + F_2 \left(\frac{q^2}{m^2} \right) \frac{i\sigma^{\mu\nu}}{2m} q_\nu \right] u(p). \quad (4)$$

On one hand, one can see that the function F_1 encodes charge renormalization, which brings a scale dependence to e_q . On the other hand, F_2 has the structure of a magnetic moment, and indeed

$$g = 2 \left[1 + F_2 \left(\frac{q^2}{m^2} \right) \right]. \quad (5)$$

To one loop, only the triangular diagram of Fig. 1 contributes to F_2 and, consequently, to $(g - 2)$. Other diagrams correspond to particle-reducible corrections to the external legs and contribute only to F_1 . The one-loop contribution to F_2 is thus given by

$$i\delta\mathcal{M}^\mu = (ie_q)^3 \int_k D_{\mu\nu}(k) \bar{u}(p') \gamma^\nu S(k + p') \gamma^\mu S(k + p) \gamma^\rho u(p), \quad (6)$$

where the free fermion propagator in momentum space is $S(k) = i/(\not{k} - m + i\epsilon)$ and the gluon free propagator in momentum space in the Feynman gauge is $D_{\mu\nu}(k) = -ig_{\mu\nu} D(k)$, with $D(k) = i/(k^2 + i\epsilon)$. Here, we use the notation $\int_k \equiv \int \frac{d^4 k}{(2\pi)^4}$.

Using the standard Feynman trick of writing

$$\frac{1}{ABC} = \int_{xyz} \frac{2}{[xA + yB + zC]^3}, \quad (7)$$

where we use the following notation for the integrals in Feynman parameters,

$$\int_{.xyz} = \int_0^1 dx dy dz \delta(x + y + z - 1), \quad (8)$$

and performing usual quantum field theory manipulations, yields

$$F_2(q^2) = \frac{\alpha}{\pi} m^2 \int_{.xyz} \frac{z(1-z)}{(1-z)^2 m^2 - xyq^2}. \quad (9)$$

For an on-shell photon ($q^2 = 0$), this leads to the well-known result $F_2(0) = \alpha/2\pi$, so that $g = 2 + \alpha/2\pi$.

B. One-loop QCD correction to the photon-quark-antiquark vertex in a strong magnetic background

Let us now consider the triangle diagram depicted in Fig. 2, encoding the first QCD correction to the quark-photon vertex. In the vacuum, its result is analogous to the one discussed in the last section, except for the inclusion of the color structure of the $SU(N_c)$ group and the swapping of the electromagnetic coupling for the strong coupling $\alpha_s = g_s^2/4\pi$. This gives rise to a AMM correction of the following form:

$$a_q^{\text{vac}} \equiv F_2^{\text{vac}}(0) = \frac{\alpha_s N_c^2 - 1}{2\pi \cdot 2N_c}. \quad (10)$$

This kind of triangle diagrams describing corrections to some fermion-antifermion-boson interaction has been calculated in the presence of external magnetic field with different methods [33,35–41].

In the presence of a strong magnetic field $\mathbf{B} = B\hat{z}$, the quark fields are quantized in Landau levels. Here we adopt the Landau gauge representation [42,43], with $A^\mu = (0, 0, Bx, 0)$. So, the matrix elements for the quark field operator have the form

$$\langle 0 | \psi(\xi) | p_{\parallel}, p_y, n \rangle = f_n(p_y, \xi_{\perp}) u_n(p_{\parallel}) e^{-ip \cdot \xi_{\parallel}}, \quad (11)$$

where ξ is a spacetime coordinate four-vector and $p^\mu = (p^0, p^1, p^2, p^3)$ is the four-momentum. The parallel and

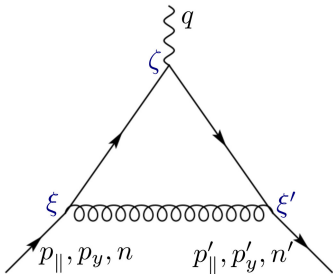


FIG. 2. One-loop QCD correction to the vertex triangular diagram that contributes to F_2 .

perpendicular vectors are defined with respect to the magnetic field direction, $\mathbf{B} = B\hat{z}$: $v_{\parallel} = (v^0, 0, 0, v^3)$ and $v_{\perp} = (0, v^1, v^2, 0)$. Also, n denotes the index of Landau levels, u is the spinor, and f_n is a diagonal matrix in spinorial space related to the solution of the Dirac equation in the presence of a magnetic background [43]. For the external photon leg, the associated photon field matrix element reads

$$\langle 0 | \mathcal{A}_\mu(\xi) | q \rangle = \varepsilon_\mu(q) e^{-iq \cdot \xi}, \quad (12)$$

where ξ_μ is a spacetime coordinate, q_μ is the four-momentum, and ε_μ is the polarization vector.

We use the Minkowski metric with an explicit separation of parallel and perpendicular components defined as $g_{\mu\nu} = g_{\mu\nu}^{\parallel} + g_{\mu\nu}^{\perp}$, where $g_{\mu\nu}^{\parallel} \equiv \text{diag}(1, 0, 0, -1)$ and $g_{\mu\nu}^{\perp} \equiv \text{diag}(0, -1, -1, 0)$. This means that for any vector $v_{\perp}^2 = -\mathbf{v}_{\perp}^2$. Also, we use a general notation for four-vector coordinates $(v^0, v^1, v^2, v^3) = (v_t, v_x, v_y, v_z)$. The temporal components of the relevant external momenta are given by

$$p_0 = \sqrt{p_z^2 + 2n\ell_q^{-2} + m^2}, \quad (13)$$

$$p'_0 = \sqrt{p_z'^2 + 2n'\ell_q^{-2} + m^2}, \quad (14)$$

$$q_0 = |q|, \quad (15)$$

where $\ell_q = |e_q B|^{-1/2}$ is the magnetic length and m is the quark mass.

The one-loop vertex transfer matrix associated with the QCD correction to the quark-photon vertex is then

$$\begin{aligned} \mathcal{T} = & -e_q g_s^2 \sum_{l,l'} \int_{\xi\xi'\zeta} e^{i(p' \cdot \xi'_{\parallel} - p \cdot \xi_{\parallel} - q \cdot \zeta)} \bar{D}_{\nu\rho}(\xi - \xi') \\ & \times \bar{u}_{n'}(p'_{\parallel}) f_{n'}^{\dagger}(p'_y, \xi'_{\perp}) \gamma^{\nu} t^a \bar{G}_l(\zeta, \xi') \\ & \times \not{\xi} \bar{G}_l(\xi, \zeta) \gamma^{\rho} t^a f_n(p_y, \xi_{\perp}) u_n(p_{\parallel}), \end{aligned} \quad (16)$$

where g_s is the gauge coupling constant, t^a are Gell-mann matrices, and \bar{G}_n is the fermion Green's function in coordinate space in the presence of the external magnetic field for a given Landau level n [8]. Here, we adopt the Feynman gauge for the gluon and its propagator $\bar{D}_{\nu\rho}(x)$ in coordinate space can be expressed in terms of the Fourier transformation as

$$\bar{D}_{\nu\rho}(\xi - \xi') = g_{\nu\rho} \int_k e^{-ik \cdot (\xi - \xi')} D(k). \quad (17)$$

The quark propagator can be expressed in terms of the Fourier transformation of the parallel coordinates

$$\bar{G}_n(\xi, \zeta) = \int_{k_{\parallel}} e^{-ik \cdot (\xi - \zeta)_{\parallel}} G_n(k_{\parallel}; \xi_{\perp}, \zeta_{\perp}), \quad (18)$$

so that, after integrating over parallel variables, we obtain parallel momentum conservation only. Therefore, we define the resulting one-loop QCD correction to the vertex matrix as

$$\mathcal{T} = (2\pi)^2 \delta^{(2)}(q_{\parallel} - p'_{\parallel} + p_{\parallel}) \varepsilon_{\mu} \delta \mathcal{M}^{\mu}, \quad (19)$$

with

$$\begin{aligned} \delta \mathcal{M}^{\mu} = & -e_q g_s^2 \frac{N_c^2 - 1}{2N_c} \int_{\xi_{\perp} \xi'_{\perp} \zeta_{\perp} k} e^{-ik \cdot (\xi - \xi')_{\perp}} D(k) \\ & \times \bar{u}'_n(p'_{\parallel}) f_n^{\dagger}(p'_y, \xi') \gamma^{\nu} G_n(k_{\parallel} + p'_{\parallel}; \zeta_{\perp}, \xi'_{\perp}) \\ & \times \gamma^{\mu} G_n(k_{\parallel} + p_{\parallel}; \xi_{\perp}, \zeta_{\perp}) \gamma_{\nu} f_n(p_y, \xi) u_n(p_{\parallel}). \end{aligned} \quad (20)$$

If we restrict our analysis to extreme magnetic fields, we can keep only the lowest-Landau level (LLL) and set $n = n' = l = l' = 0$. Then, our expressions simplify to

$$f_0(p_y, \xi_{\perp}) u_0(p_{\parallel}) = u_0(p_{\parallel}) \frac{e^{ip_y \xi_y - \frac{1}{2}(\xi_x/\ell_q + sp_y \ell_q)^2}}{(\pi \ell_q^2)^{1/4}}, \quad (21)$$

$$\begin{aligned} \mathcal{F} = & \frac{e_q g_s^2}{3\ell_q^5 \pi^{5/2}} \int_{\xi_{\perp} \xi'_{\perp} \zeta_{\perp}} \exp \left\{ -ik \cdot (\xi - \xi')_{\perp} + ip_y \xi_y - ip'_y \xi'_y + \frac{(\zeta - \xi)_{\perp}^2}{4\ell_q^2} + \frac{(\xi' - \zeta)_{\perp}^2}{4\ell_q^2} \right. \\ & \left. - \frac{1}{2}(\xi_x/\ell_q + sp_y \ell_q)^2 - \frac{1}{2}(\xi'_x/\ell_q + sp'_y \ell_q)^2 - \frac{is}{2\ell_q^2}(\xi_x + \zeta_x)(\xi_y - \zeta_y) - \frac{is}{2\ell_q^2}(\zeta_x + \xi'_x)(\zeta_y - \xi'_y) \right\}, \end{aligned} \quad (24)$$

$$\mathcal{G}^{\mu} = - \int_{k_{\parallel}} D(k) \bar{u}_0(p'_{\parallel}) \gamma^{\nu} S(k_{\parallel} + p'_{\parallel}) \mathcal{P}_+ \gamma^{\mu} S(k_{\parallel} + p_{\parallel}) \mathcal{P}_+ \gamma_{\nu} u_0(p_{\parallel}). \quad (25)$$

The integrals in \mathcal{F} are Gaussian and can be evaluated analytically. After a long but straightforward calculation, Eq. (23) is reduced to

$$\delta \mathcal{M}_{\text{LLL}}^{\mu} = \frac{4}{3} e_q g_s^2 \int_{k_{\perp}} e^{\frac{1}{2} k_{\perp}^2 \ell_q^2} \mathcal{G}^{\mu}(p_{\parallel}, p'_{\parallel}, k_{\perp}). \quad (26)$$

Notice that the dependence in p_y and p'_y disappears. Because of the projectors \mathcal{P}_{\pm} in Eq. (25), the perpendicular components of \mathcal{G}^{μ} vanish and the form factors are restricted only to the parallel directions, i.e., $\mu = 0$ and $\mu = 3$. Moreover, there is only dependence on parallel momenta, so that all vectors and tensors will be reduced to their parallel components.

The detailed calculation of \mathcal{G}^{μ} is long, but straightforward, and the full result is not particularly illuminating. In the end, there are two terms related to F_2 that are proportional to $\sigma_{\parallel}^{\mu\nu} q_{\nu}$ and $\gamma_1 \gamma_2 \sigma_{\parallel}^{\mu\nu} q_{\nu}$.

C. Implications to the AMM

The AMM is better described by the polarization projections $\mathcal{P}_+ \sigma_{\parallel}^{\mu\nu} q_{\nu}$ and $\mathcal{P}_- \sigma_{\parallel}^{\mu\nu} q_{\nu}$. Defining $\delta \mathcal{M}_{\text{LLL}}^{\mu} = \delta \mathcal{M}_+^{\mu} + \delta \mathcal{M}_-^{\mu}$

$$\begin{aligned} G_0(k_{\parallel}; \zeta_{\perp}, \xi_{\perp}) = & \frac{i}{2\pi \ell_q^2} S(k_{\parallel}) \mathcal{P}_+ \\ & \times e^{\frac{is}{2\ell_q^2}(\xi_x + \zeta_x)(\xi_y - \zeta_y)} e^{\frac{1}{4\ell_q^2}(\zeta_{\perp} - \xi_{\perp})^2}, \end{aligned} \quad (22)$$

where $s = \text{sgn}(e_q B)$, and we have defined the projectors $\mathcal{P}_{\pm} = \frac{1}{2}[1 \pm si\gamma_1\gamma_2]$ or, equivalently, $\mathcal{P}_{\pm} = \frac{1}{2}[1 \pm \Sigma_3]$, with $\Sigma_3 = \text{diag}(1, -1, 1, -1)$ being the third component of the spin projection (cf. also Ref. [8]). The Schwinger phase corresponds to the first exponential in the second line of Eq. (22).

The LLL matrix can be separated in parallel and perpendicular integrals in the following form:

$$\delta \mathcal{M}_{\text{LLL}}^{\mu} = \int_{k_{\perp}} \mathcal{F}(p_y, p'_y, k_{\perp}) \mathcal{G}^{\mu}(p_{\parallel}, p'_{\parallel}, k_{\perp}^2), \quad (23)$$

with

and using $\bar{u}_0(p'_{\parallel})(p'_{\parallel} - m) = 0$, $(p'_{\parallel} - m) \times u_0(p_{\parallel}) = 0$ and the Gordon identity, we obtain the following structure:

$$\delta \mathcal{M}_{\pm}^{\mu} = e_q \bar{u}_0(p'_{\parallel}) \left[\delta F_1^{\pm} \gamma_{\parallel}^{\mu} + F_2^{\pm} \sigma_{\parallel}^{\mu\nu} \frac{i q_{\nu}}{2m} + F_3^{\pm} q_{\parallel}^{\mu} \right] \mathcal{P}_{\pm} u_0(p_{\parallel}), \quad (27)$$

so that the AMM splits in the two polarization projections.

Here, δF_1 represents a correction to the tree level charge vertex. All the form factors F_i are functions of q_{\parallel}^2/m^2 . F_2 can be recognized as the AMM contribution, but projected onto parallel components only. The third term F_3 should be interpreted as a correction to the term $\partial \cdot A_{\parallel}$, related to the gauge fixing.

In summary, if we consider the full magnetic moment, we have the following modification in the presence of a very large magnetic background:

$$(1 + a) \sigma_{\mu\nu} F^{\mu\nu} \rightarrow \sum_{s=\pm} (\sigma_{\mu\nu} F^{\mu\nu} + a^s \sigma_{\mu\nu}^{\parallel} F_{\parallel}^{\mu\nu}) \mathcal{P}_s, \quad (28)$$

where the parallel-project AMM contributes as $\sim iE_3\sigma_3$. This term, however, should not be confused with an anomalous electric dipole moment [34]. The other AMM contributions to $\mathbf{B} \cdot \boldsymbol{\sigma}$ and $i\mathbf{E} \cdot \boldsymbol{\sigma}_\perp$ are completely suppressed. Indeed, this becomes clear when the corrections are written in matrix form:

$$\sum_{s=\pm} a^s \sigma_{\mu\nu}^{\parallel} F_{\parallel}^{\mu\nu} \mathcal{P}_s = -2iE_z \text{diag}(a^+, -a^-, -a^+, a^-), \quad (29)$$

when compared to the standard anomalous term in vacuum:

$$a \sigma_{\mu\nu} F^{\mu\nu} = -2a \begin{pmatrix} \mathbf{B} \cdot \boldsymbol{\sigma} + i\mathbf{E} \cdot \boldsymbol{\sigma}_\perp & 0 \\ 0 & \mathbf{B} \cdot \boldsymbol{\sigma} - i\mathbf{E} \cdot \boldsymbol{\sigma}_\perp \end{pmatrix} - 2iE_z \text{diag}(a, -a, -a, a). \quad (30)$$

Furthermore, since in general $a^+ \neq a^-$, an asymmetry between the spin up and spin down corrections develops in the presence of a very large magnetic background.

Integrating over inner parallel momenta with the use of Feynman parameters, the AMM component of Eq. (27) reads

$$F_2^\pm(q_{\parallel}^2) = \int_{xyz} \int_{k_\perp} \frac{\frac{4}{3} g_s^2 e^{-\frac{1}{2} k_\perp^2 \ell_q^2} m^2 f^\pm(z) / 4\pi}{[m^2(1-z)^2 - q_{\parallel}^2 xy + (\mathbf{k}_\perp^2 + m_g^2)z]^2}, \quad (31)$$

where

$$f^+(z) = \frac{2}{3}(1 + 6z) \quad (32)$$

$$f^-(z) = z(4 - z) - \frac{2}{3}. \quad (33)$$

To avoid anticipated infrared divergences, we simply add a mass term m_g to the gluon propagator, leaving the discussion of possible physical choices and their consequences to the next subsection.

Since the form factors F_i depend on q_{\parallel}^2 , we can choose a frame where $q_{\parallel}^2 = 0$ if $p_z = p'_z$ or, in the ultrarelativistic case, for aligned $p_z \gg m$ and $p'_z \gg m$. In this frame, it is easy to integrate over two of the three Feynman parameters. On the other hand, the perpendicular momentum integral can be evaluated in polar coordinates. Changing variables as $|\mathbf{k}_\perp|^2 = 2m^2\eta$, we obtain

$$\begin{aligned} a_q^\pm &\equiv F_2^\pm(0) \\ &= a_q^{\text{vac}} \int_0^1 dz \int_0^\infty d\eta \frac{e^{-(m\ell_q)^2\eta} f^\pm(z)(1-z)}{[(1-z)^2 + (m_g/m)^2 z + 2\eta z]^2}. \end{aligned} \quad (34)$$

One should recall [cf. Eq. (10)] that a_q^{vac} contains the strong coupling α_s which, in principle, runs with the relevant energy scale.

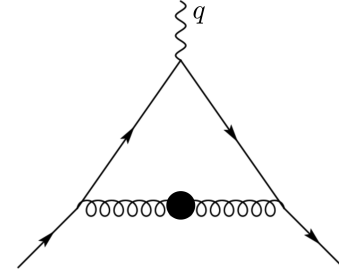


FIG. 3. One-loop QCD correction to the vertex triangular diagram with a dressed gluon propagator.

D. Effective mass for the gluons

We have introduced a mass term m_g for the gluon in the calculation of the one-loop quark-antiquark-photon vertex in the presence of an extremely large magnetic background. This scale is necessary to regulate infrared divergences that appear in this extreme limit.¹ We shall analyze the results in two different scenarios that we motivate in what follows: (i) a fixed scale and (ii) a magnetically-dressed gluon self-energy as shown diagrammatically in Fig. 3.

First, we consider a fixed infrared scale $m_g \sim 0.3$ GeV inspired by results for correlation functions in the non-perturbative region of QCD (and in associated pure gauge theories). For Landau and linear covariant gauges, different lattice simulations [44–47], Schwinger-Dyson equations [48–50], and infrared models [51–53] seem to indicate the emergence of an infrared mass scale of this order.

Second, we analyze the consequences of the intense magnetic background on the gluon polarization tensor to introduce a magnetically dressed gluon in our triangle diagram computation. Following [54–57], the gluon polarization tensor in the presence of an intense magnetic field, i.e. within the LLL approximation, is transverse in the parallel components. Hence,

$$\Pi_g^{\mu\nu}(k) = \left(g_{\parallel}^{\mu\nu} - \frac{k_{\parallel}^{\mu} k_{\parallel}^{\nu}}{k_{\parallel}^2} \right) \Pi_g(k_{\parallel}^2, k_{\perp}^2), \quad (35)$$

where

$$\Pi_g(k_{\parallel}^2, k_{\perp}^2) = \frac{\alpha_s}{\pi} N_c \sum_q \frac{e^{-\frac{1}{2} \ell_q^2 k_{\perp}^2}}{\pi^2 \ell_q^2} g(m_q^2/k_{\parallel}^2). \quad (36)$$

We shall adopt the chiral-limit approximation $g(m^2/k_{\parallel}^2) \approx g(0) = 1$, so that the remaining dependence is on the perpendicular component of the momentum. Notice that the polarization factor is exponentially suppressed

¹It is important to note that, in this regime, the QED triangle diagram also displays the same infrared divergences and the full AMM calculation at one loop would also require an IR regularization for the photon that we do not discuss here.

for $k_{\perp}^2 > |eB|$. We will consider then Π_g as a magnetically dressed gluon squared mass.

III. QCD CORRECTION TO THE AMM AS A FUNCTION OF THE MAGNETIC FIELD

Now we proceed to the numerical analysis of the behavior of the one-loop QCD correction to the AMM in the presence of a very strong magnetic background, a_q^{\pm} , compared with its vacuum counterpart, a_q^{vac} , as defined in Eqs. (34) and (10), respectively. In this analysis, we consider the two scenarios for the effective gluon mass discussed in the previous section: a constant gluon mass, which we take as $m_g = 0.3$ GeV, and one given by the LLL polarization tensor, $m_g^2 = \Pi_g$, as defined in Eq. (36). In both cases we investigate what happens if we set the renormalization scale to run with the magnetic field, $\mu_{\overline{\text{MS}}} = \sqrt{|eB|}$, or to a fixed value, $\mu_{\overline{\text{MS}}} = 1$ GeV.

Figure 4 shows the case with a fixed gluon mass, $m_g = 0.3$ GeV, and $\mu_{\overline{\text{MS}}} = \sqrt{|eB|}$. The first thing to be noticed is the change of sign of the polarization components of the AMM, being a_q^+ positive and a_q^- negative. Moreover, we find that $a_q^- \approx -a_q^+$, within $\sim 1\%$. One can also see that $|a_u^{\pm}| > |a_d^{\pm}|$. This happens because the quark charge, through ℓ_q , dominates in the exponential term in Eq. (34). The plots present an increase in $|a_q^{\pm}|$ as a function of eB . In fact, $|a_u^{\pm}|$ is greater than its corresponding vacuum value for $eB \gtrsim 2$ GeV², and $|a_d^{\pm}|$ is greater than its vacuum value for $eB \gtrsim 4$ GeV². This growth in the ratio $a_q^{\pm}/a_q^{\text{vac}}$ is, however, somewhat misleading. It basically represents the running of α_s with the magnetic field in the denominator of the ratio. a_q^{\pm} is, indeed, almost constant, as can be seen in Fig. 5.

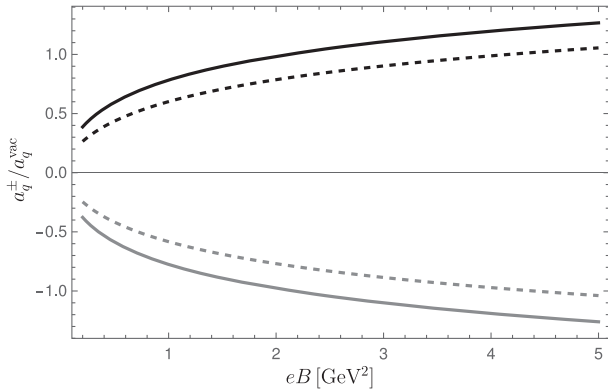


FIG. 4. Anomalous magnetic moments a_u^+ (black solid), a_u^- (gray solid), a_d^+ (black dashed), and a_d^- (gray dashed), scaled by their values in the vacuum, as functions of the external magnetic field. Here we consider dressed gluons with $m_g = 0.3$ GeV and a renormalization scale $\mu_{\overline{\text{MS}}} = \sqrt{|eB|}$.

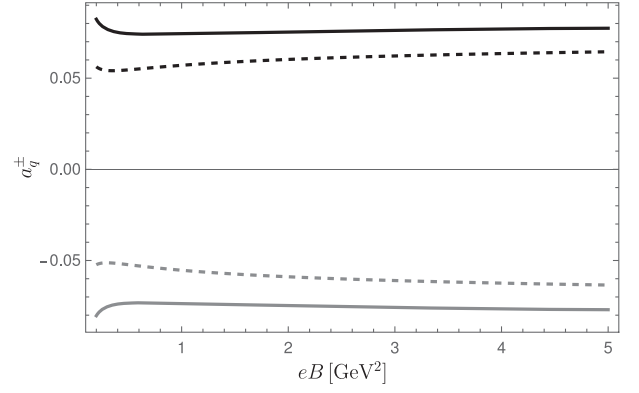


FIG. 5. Anomalous magnetic moments a_u^+ (black solid), a_u^- (gray solid), a_d^+ (black dashed), and a_d^- (gray dashed), as functions of the external magnetic field. Here we consider dressed gluons with $m_g = 0.3$ GeV and a renormalization scale $\mu_{\overline{\text{MS}}} = \sqrt{|eB|}$.

The behavior of the ratio $a_q^{\pm}/a_q^{\text{vac}}$ for a fixed scale $\mu_{\overline{\text{MS}}} = 1$ GeV is basically the same, since the main changes are contained in the global factor $\sim \alpha_s$. The modifications in the running quark mass have no significant impact, producing differences of $\sim 0.1\%$.

Since we consider an effective nonperturbative gluon mass of 0.3 GeV, we also show the analogous results for a constituent quark mass of $m_q = 0.35$ GeV in Figs. 6 and 7. The larger quark mass brings no remarkable qualitative modification, yielding approximately a shift in the positive direction.

A totally different outcome occurs when we consider the dressed gluon mass as given by the LLL polarization tensor, $m_g^2 = \Pi_g$, and a renormalization scale $\mu_{\overline{\text{MS}}} = \sqrt{|eB|}$. Contrary to what happens for a constant gluon mass, the absolute value of the AMM now diminishes as the magnetic field increases, as illustrated in Fig. 8.

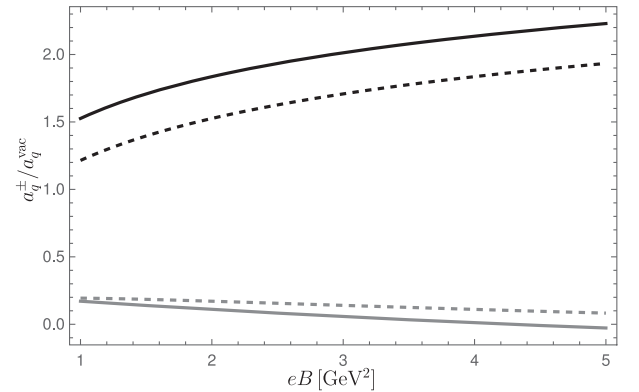


FIG. 6. Anomalous magnetic moments a_u^+ (black solid), a_u^- (gray solid), a_d^+ (black dashed), and a_d^- (gray dashed), scaled by their values in the vacuum, as functions of the external magnetic field. Here we consider dressed gluons and quarks with $m_g = 0.3$ and $m_q = 0.35$ GeV.

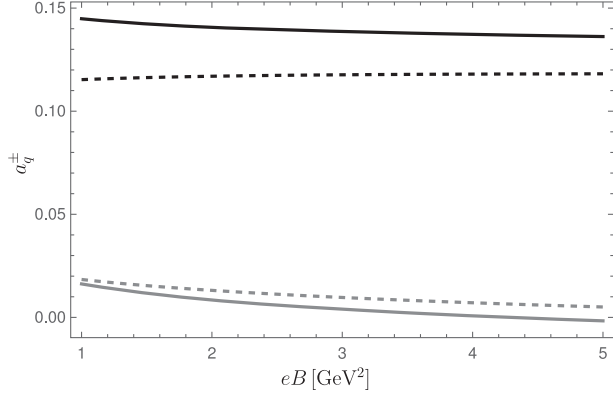


FIG. 7. Anomalous magnetic moments a_u^+ (black solid), a_u^- (gray solid), a_d^+ (black dashed), and a_d^- (gray dashed), scaled by their values in the vacuum, as functions of the external magnetic field. Here we consider dressed gluons and quarks with $m_g = 0.3$ and $m_q = 0.35$ GeV, and with the renormalization scale $\mu_{\overline{\text{MS}}} = \sqrt{|eB|}$.

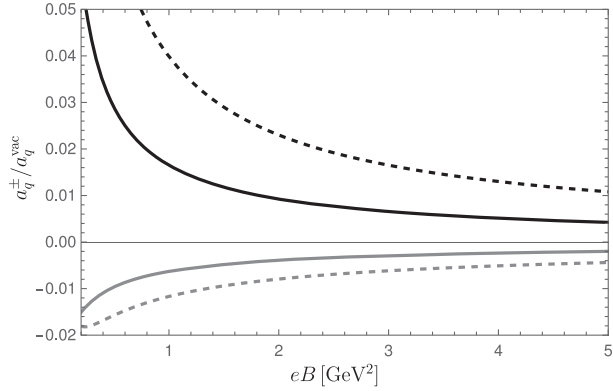


FIG. 8. Anomalous magnetic moments a_u^+ (black solid), a_u^- (gray solid), a_d^+ (black dashed), and a_d^- (gray dashed), scaled by their values in the vacuum, as functions of the external magnetic field. Here we consider dressed gluons with $m_g^2 = \Pi_g$ and a renormalization scale $\mu_{\overline{\text{MS}}} = \sqrt{|eB|}$.

This behavior is expected since Π_g grows with the magnetic field. If we consider a fixed renormalization scale, $\mu_{\overline{\text{MS}}} = 1$ GeV, the plot looks very similar. However, the difference is larger than in the case of a fixed gluon mass. The difference between the two cases increases $\sim 10\%$ for $eB \sim 5$ GeV² but stabilizes at higher values.

The strong magnetic background effects on the electron AMM are, of course, analogous. One has only to substitute the running strong coupling by the electromagnetic

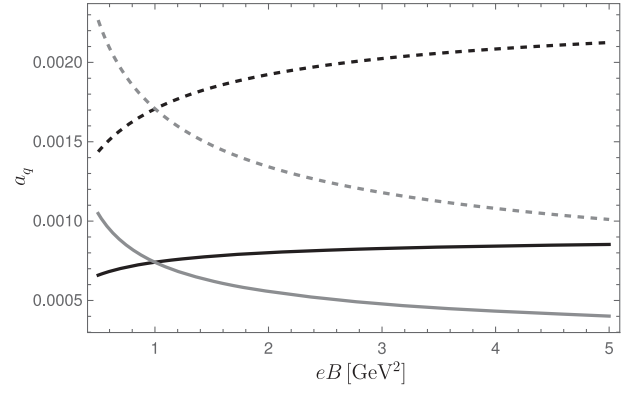


FIG. 9. Total anomalous magnetic moments $a_u = a_u^+ + a_u^-$ (solid), and $a_d = a_d^+ + a_d^-$ (dashed), as functions of the external magnetic field. Here we consider dressed gluons with $m_g = 0.3$ GeV, current quark masses, and the renormalization scales $\mu_{\overline{\text{MS}}} = \sqrt{|eB|}$ (gray) and $\mu_{\overline{\text{MS}}} = 1$ GeV (black).

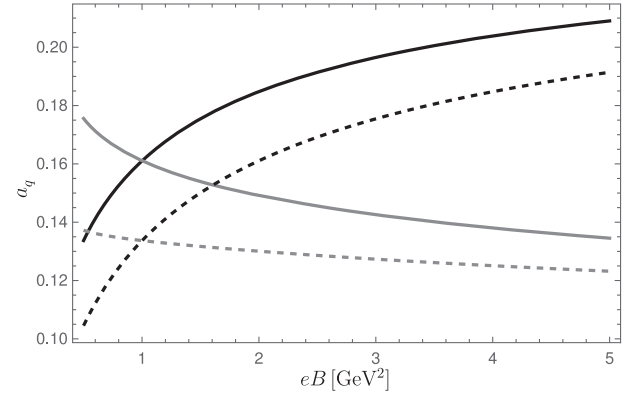


FIG. 10. Total anomalous magnetic moments $a_u = a_u^+ + a_u^-$ (solid), and $a_d = a_d^+ + a_d^-$ (dashed), as functions of the external magnetic field. Here we consider dressed gluons with $m_g = 0.3$ GeV, $m_q = 0.35$ GeV, and the renormalization scales $\mu_{\overline{\text{MS}}} = \sqrt{|eB|}$ (gray) and $\mu_{\overline{\text{MS}}} = 1$ GeV (black).

coupling and set the global factor $(N_c^2 - 1)/2N_c \rightarrow 1$ in Eq. (10), besides considering one flavor with charge e and with $N_c \rightarrow 1$ in Eq. (36).

The total anomalous magnetic moments, $a_u = a_u^+ + a_u^-$ and $a_d = a_d^+ + a_d^-$, as functions of the external magnetic field are shown in Figs. 9–11 for the three cases considered above. As previously, remarkable qualitative modifications occur only when we consider the dressed gluon mass as given by $m_g^2 = \Pi_g$ and a renormalization scale $\mu_{\overline{\text{MS}}} = \sqrt{|eB|}$, where the absolute value of the total AMM diminishes as the magnetic field increases.

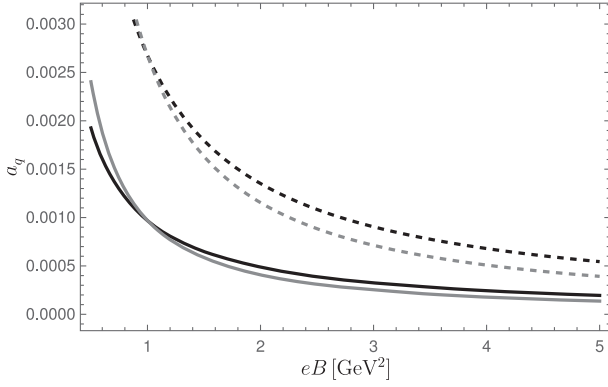


FIG. 11. Total anomalous magnetic moments $a_u = a_u^+ + a_u^-$ (solid), and $a_d = a_d^+ + a_d^-$ (dashed), as functions of the external magnetic field. Here we consider dressed gluons with $m_g^2 = \Pi_g$, current quark masses, and the renormalization scales $\mu_{\overline{\text{MS}}} = \sqrt{|eB|}$ (gray) and $\mu_{\overline{\text{MS}}} = 1 \text{ GeV}$ (black).

IV. SUMMARY AND OUTLOOK

In this paper we computed the part relevant to the quark AMM of the one-loop QCD correction to the photon-quark-antiquark vertex in an extremely strong magnetic background, i.e., one in which \sqrt{eB} is much larger than all other mass scales. This justified the use of the lowest-Landau level approximation. The solution exhibits infrared divergences. These can be tamed by attributing an effective mass to gluons that acts as an infrared regulator, inspired by what is expected to happen in the infrared sector of strong interactions [58]. In this vein, we considered two standard scenarios: one with a constant gluon mass, $m_g = 0.3 \text{ GeV}$, which sits in the ballpark of Λ_{QCD} , and one in which the gluon mass comes from the one-loop correction to its polarization tensor in the presence of an external magnetic field in the LLL approximation, $m_g^2 = \Pi_g$. In both cases we investigated what happens if we set the renormalization scale to run with the magnetic field, $\mu_{\overline{\text{MS}}} = \sqrt{|eB|}$, or to a fixed value, $\mu_{\overline{\text{MS}}} = 1 \text{ GeV}$.

It has been previously shown that the AMM is induced by chiral symmetry breaking, being related to a non-perturbative contribution [59,60]. In our calculation, the AMM also vanishes in the chiral limit. However, in our case we consider only perturbative vertex corrections. So, when spontaneous symmetry breaking occurs, the generation of an AMM is indeed expected. The previous references consider Schwinger-Dyson equations which in fact incorporate nonperturbative effects. This could be introduced here through operator product expansion as a nonperturbative effect, which is out of the scope of the present analysis.

Considering the total magnetic moment, we found that it is such that the anomalous magnetic moment contributes to the electric part $\sim iE_3\sigma_3$, the other contributions to $\mathbf{B} \cdot \boldsymbol{\sigma}$ and $i\mathbf{E} \cdot \boldsymbol{\sigma}_\perp$ being completely suppressed. We found that the anomalous contribution can be naturally separated into two polarization projections obtained from $\mathcal{P}_\pm = \frac{1}{2}(1 \pm is\gamma_1\gamma_2)$, or equivalently $\frac{1}{2}(1 + \Sigma_3)$.

We presented results for the behavior of the anomalous magnetic moment of quarks up and down, scaled by their values in the vacuum, as a function of the external magnetic field, for the choices of gluon mass and renormalization scale discussed above. We found that the case with a fixed gluon mass exhibits an increase of the ratio a^\pm/a_{vac} , while this observable in the case with gluon mass given by $m_g^2 = \Pi_g$ decreases as the magnetic field increases. The latter setup, which seems to be closer to a more physical description of the gluon mass, shows a strong suppression, i.e., the quark AMM apparently vanishes for extremely large magnetic fields.

We also found asymmetry between spin up and spin down components of the anomalous correction, which might be more promising in searching possible experimental observables.

A natural extension of the treatment presented here would be considering the case with other Landau levels in the external lines of the triangular diagram. This would bring information on the interplay between different levels in the computation of the quark anomalous magnetic moment.

One could also incorporate effects from a thermal or dense medium to the framework discussed here. To do that, one would need to consider hot and dense magnetic QCD [37,41,61–64] in the computation of the photon-quark-antiquark vertex. The thermal case could be relevant for high-energy heavy-ion collisions, and even play a role in the chiral magnetic effect scenario, since the quark AMM could destroy the fermion zero mode in the presence of a magnetic field. The case at high densities is of interest in magnetars, where ultrahigh magnetic fields can also be achieved. Although in this case the effect on the equation of state seems to be minor [18], it contributes to increase the level of pressure anisotropy [16]. Finally, a calculation of the quark AMM within lattice QCD in the presence of a strong magnetic background would provide a clean benchmark.

ACKNOWLEDGMENTS

This work was partially supported by CAPES (Finance Code 001), CNPq, FAPERJ, INCT-FNA (Process No. 464898/2014-5), and ANID/FONDECYT under Grant No. 1190192.

- [1] J. S. Schwinger, On quantum electrodynamics and the magnetic moment of the electron, *Phys. Rev.* **73**, 416 (1948).
- [2] T. Aoyama, T. Kinoshita, and M. Nio, Theory of the anomalous magnetic moment of the electron, *Atoms* **7**, 28 (2019).
- [3] J. S. Schwinger, Quantum electrodynamics. III: The electromagnetic properties of the electron: Radiative corrections to scattering, *Phys. Rev.* **76**, 790 (1949).
- [4] J. S. Schwinger, On gauge invariance and vacuum polarization, *Phys. Rev.* **82**, 664 (1951).
- [5] V. N. Baier, V. M. Katkov, and V. M. Strakhovenko, Anomalous magnetic moment of the electron in the magnetic field, *Yad. Fiz.* **24**, 379 (1976).
- [6] V. N. Baier and V. M. Katkov, Anomalous magnetic moment of the electron in a medium, *Phys. Lett. A* **280**, 275 (2001).
- [7] V. P. Gusynin, V. A. Miransky, and I. A. Shovkovy, Dimensional reduction and catalysis of dynamical symmetry breaking by a magnetic field, *Nucl. Phys.* **B462**, 249 (1996).
- [8] I. A. Shovkovy, Magnetic catalysis: A review, *Lect. Notes Phys.* **871**, 13 (2013).
- [9] V. A. Miransky and I. A. Shovkovy, Quantum field theory in a magnetic field: From quantum chromodynamics to graphene and Dirac semimetals, *Phys. Rep.* **576**, 1 (2015).
- [10] K. Fukushima, D. E. Kharzeev, and H. J. Warringa, The chiral magnetic effect, *Phys. Rev. D* **78**, 074033 (2008).
- [11] D. E. Kharzeev, L. D. McLerran, and H. J. Warringa, The effects of topological charge change in heavy ion collisions: Event by event P and CP violation, *Nucl. Phys.* **A803**, 227 (2008).
- [12] V. Skokov, A. Y. Illarionov, and V. Toneev, Estimate of the magnetic field strength in heavy-ion collisions, *Int. J. Mod. Phys. A* **24**, 5925 (2009).
- [13] W.-T. Deng and X.-G. Huang, Event-by-event generation of electromagnetic fields in heavy-ion collisions, *Phys. Rev. C* **85**, 044907 (2012).
- [14] P. J. A. Bicudo, J. E. F. T. Ribeiro, and R. Fernandes, The Anomalous magnetic moment of quarks, *Phys. Rev. C* **59**, 1107 (1999).
- [15] E. J. Ferrer and V. de la Incera, Dynamically generated anomalous magnetic moment in massless QED, *Nucl. Phys.* **B824**, 217 (2010).
- [16] M. Strickland, V. Dexheimer, and D. P. Menezes, Bulk properties of a Fermi gas in a magnetic field, *Phys. Rev. D* **86**, 125032 (2012).
- [17] S. Fayazbakhsh and N. Sadooghi, Anomalous magnetic moment of hot quarks, inverse magnetic catalysis, and reentrance of the chiral symmetry broken phase, *Phys. Rev. D* **90**, 105030 (2014).
- [18] E. J. Ferrer, V. de la Incera, D. Manreza Paret, A. Pérez Martínez, and A. Sanchez, Insignificance of the anomalous magnetic moment of charged fermions for the equation of state of a magnetized and dense medium, *Phys. Rev. D* **91**, 085041 (2015).
- [19] S. Mao and D. H. Rischke, Dynamically generated magnetic moment in the Wigner-function formalism, *Phys. Lett. B* **792**, 149 (2019).
- [20] N. Chaudhuri, S. Ghosh, S. Sarkar, and P. Roy, Effect of the anomalous magnetic moment of quarks on the phase structure and mesonic properties in the NJL model, *Phys. Rev. D* **99**, 116025 (2019).
- [21] M. Coppola, D. Gomez Dumm, S. Noguera, and N. N. Scoccola, Neutral and charged pion properties under strong magnetic fields in the NJL model, *Phys. Rev. D* **100**, 054014 (2019).
- [22] J. Mei and S. Mao, Inverse catalysis effect of the quark anomalous magnetic moment to chiral restoration and deconfinement phase transitions, *Phys. Rev. D* **102**, 114035 (2020).
- [23] N. Chaudhuri, S. Ghosh, S. Sarkar, and P. Roy, Effects of quark anomalous magnetic moment on the thermodynamical properties and mesonic excitations of magnetized hot and dense matter in PNJL model, *Eur. Phys. J. A* **56**, 213 (2020).
- [24] S. Ghosh, N. Chaudhuri, S. Sarkar, and P. Roy, Effects of the anomalous magnetic moment of quarks on the dilepton production from hot and dense magnetized quark matter using the NJL model, *Phys. Rev. D* **101**, 096002 (2020).
- [25] K. Xu, J. Chao, and M. Huang, Effect of the anomalous magnetic moment of quarks on magnetized QCD matter and meson spectra, *Phys. Rev. D* **103**, 076015 (2021).
- [26] S. Ghosh, N. Chaudhuri, P. Roy, and S. Sarkar, Thermomagnetic modification of the anomalous magnetic moment of quarks using the NJL model, *Phys. Rev. D* **103**, 116008 (2021).
- [27] R. L. S. Farias, W. R. Tavares, R. M. Nunes, and S. S. Avancini, Effects of the quark anomalous magnetic moment in the chiral symmetry restoration: Magnetic catalysis and inverse magnetic catalysis, *Eur. Phys. J. C* **82**, 674 (2022).
- [28] N. Chaudhuri, S. Ghosh, S. Sarkar, and P. Roy, Dilepton production from magnetized quark matter with an anomalous magnetic moment of the quarks using a three-flavor PNJL model, *Phys. Rev. D* **103**, 096021 (2021).
- [29] M. Kawaguchi and M. Huang, Restriction on the form of the quark anomalous magnetic moment from lattice QCD results, *Chin. Phys. C* **47**, 064103 (2023).
- [30] S. Mao, Inverse catalysis effect of the quark anomalous magnetic moment to chiral restoration and deconfinement phase transitions at finite baryon chemical potential, *Phys. Rev. D* **106**, 034018 (2022).
- [31] N. Chaudhuri, S. Ghosh, P. Roy, and S. Sarkar, Anisotropic pressure of magnetized quark matter with anomalous magnetic moment, *Phys. Rev. D* **106**, 056020 (2022).
- [32] W. R. Tavares, S. S. Avancini, R. L. S. Farias, and R. P. Cardoso, Artificial first-order phase transition in a magnetized Nambu–Jona-Lasinio model with a quark anomalous magnetic moment, *Phys. Rev. D* **109**, 016011 (2024).
- [33] F. Lin and M. Huang, Magnetic correction to the anomalous magnetic moment of electrons, *Commun. Theor. Phys.* **74**, 055202 (2022).
- [34] M. D. Schwartz, *Quantum Field Theory and the Standard Model* (Cambridge University Press, Cambridge, England, 2014).
- [35] A. Ayala, J. L. Hernández, L. A. Hernández, R. L. S. Farias, and R. Zamora, Magnetic corrections to the boson self-coupling and boson-fermion coupling in the linear sigma model with quarks, *Phys. Rev. D* **102**, 114038 (2020).
- [36] C. Villavicencio, Axial coupling constant in a magnetic background, *Phys. Rev. D* **107**, 076009 (2023).

- [37] C. A. Dominguez, M. Loewe, C. Villavicencio, and R. Zamora, Nucleon axial-vector coupling constant in magnetar environments, *Phys. Rev. D* **108**, 074024 (2023).
- [38] F. L. Braghin, Constituent quark-light vector mesons effective couplings in a weak background magnetic field, *Phys. Rev. D* **97**, 014022 (2018); **101**, 039902(E) (2020).
- [39] F. L. Braghin and W. F. De Sousa, Weak magnetic field corrections to pion and constituent quarks form factors, *J. Phys. G* **47**, 045110 (2020).
- [40] F. L. Braghin, M. Loewe, and C. Villavicencio, Yukawa potential under weak magnetic field, *Phys. Rev. D* **109**, 034014 (2024).
- [41] C. A. Dominguez, M. Loewe, C. Villavicencio, and R. Zamora, Magnetic and density effects on the nucleon axial coupling, in *26th High-Energy Physics International Conference in QCD* (2023), [arXiv:2309.05807](https://arxiv.org/abs/2309.05807).
- [42] A. J. Parle, Quantum electrodynamics in strong magnetic fields. 4. Electron self-energy, *Aust. J. Phys.* **40**, 1 (1987).
- [43] P. Elmfors, D. Persson, and B.-S. Skagerstam, Thermal fermionic dispersion relations in a magnetic field, *Nucl. Phys.* **B464**, 153 (1996).
- [44] A. Cucchieri and T. Mendes, What's up with IR gluon and ghost propagators in Landau gauge? A puzzling answer from huge lattices, *Proc. Sci. LATTICE2007* (2007) 297 [[arXiv:0710.0412](https://arxiv.org/abs/0710.0412)].
- [45] I. L. Bogolubsky, E. M. Ilgenfritz, M. Muller-Preussker, and A. Sternbeck, The Landau gauge gluon and ghost propagators in 4D SU(3) gluodynamics in large lattice volumes, *Proc. Sci. LATTICE2007* (2007) 290 [[arXiv:0710.1968](https://arxiv.org/abs/0710.1968)].
- [46] O. Oliveira and P. Bicudo, Running gluon mass from Landau gauge lattice QCD propagator, *J. Phys. G* **38**, 045003 (2011).
- [47] P. Bicudo, D. Binosi, N. Cardoso, O. Oliveira, and P. J. Silva, Lattice gluon propagator in renormalizable ξ gauges, *Phys. Rev. D* **92**, 114514 (2015).
- [48] A. C. Aguilar, D. Binosi, and J. Papavassiliou, Gluon and ghost propagators in the Landau gauge: Deriving lattice results from Schwinger-Dyson equations, *Phys. Rev. D* **78**, 025010 (2008).
- [49] N. Mueller, J. A. Bonnet, and C. S. Fischer, Dynamical quark mass generation in a strong external magnetic field, *Phys. Rev. D* **89**, 094023 (2014).
- [50] A. C. Aguilar, D. Binosi, and J. Papavassiliou, The gluon mass generation mechanism: A concise primer, *Front. Phys. (Beijing)* **11**, 111203 (2016).
- [51] D. Dudal, J. A. Gracey, S. P. Sorella, N. Vandersickel, and H. Verschelde, A refinement of the Gribov-Zwanziger approach in the Landau gauge: Infrared propagators in harmony with the lattice results, *Phys. Rev. D* **78**, 065047 (2008).
- [52] M. A. L. Capri, D. Dudal, D. Fiorentini, M. S. Guimaraes, I. F. Justo, A. D. Pereira, B. W. Mintz, L. F. Palhares, R. F. Sobreiro, and S. P. Sorella, Exact nilpotent nonperturbative BRST symmetry for the Gribov-Zwanziger action in the linear covariant gauge, *Phys. Rev. D* **92**, 045039 (2015).
- [53] M. Peláez, U. Reinosa, J. Serreau, M. Tissier, and N. Wschebor, A window on infrared QCD with small expansion parameters, *Rep. Prog. Phys.* **84**, 124202 (2021).
- [54] K. Fukushima, Magnetic-field induced screening effect and collective excitations, *Phys. Rev. D* **83**, 111501 (2011).
- [55] A. Bandyopadhyay, C. A. Islam, and M. G. Mustafa, Electromagnetic spectral properties and Debye screening of a strongly magnetized hot medium, *Phys. Rev. D* **94**, 114034 (2016).
- [56] A. Ayala, J. D. Castaño Yepes, C. A. Dominguez, S. Hernández-Ortiz, L. A. Hernández, M. Loewe, D. Manreza Paret, and R. Zamora, Thermal corrections to the gluon magnetic Debye mass, *Rev. Mex. Fis.* **66**, 446 (2020).
- [57] A. Ayala, J. D. Castaño Yepes, M. Loewe, and E. Muñoz, Gluon polarization tensor in a magnetized medium: Analytic approach starting from the sum over Landau levels, *Phys. Rev. D* **101**, 036016 (2020).
- [58] C. Mena and L. F. Palhares, Quark-photon vertex in confining models, [arXiv:2311.14178](https://arxiv.org/abs/2311.14178).
- [59] E. J. Ferrer and V. de la Incera, Dynamically induced Zeeman effect in massless QED, *Phys. Rev. Lett.* **102**, 050402 (2009).
- [60] L. Chang, Y.-X. Liu, and C. D. Roberts, Dressed-quark anomalous magnetic moments, *Phys. Rev. Lett.* **106**, 072001 (2011).
- [61] J.-P. Blaizot, E. S. Fraga, and L. F. Palhares, Effect of quark masses on the QCD pressure in a strong magnetic background, *Phys. Lett. B* **722**, 167 (2013).
- [62] A. Ayala, L. A. Hernández, M. Loewe, and C. Villavicencio, QCD phase diagram in a magnetized medium from the chiral symmetry perspective: The linear sigma model with quarks and the Nambu–Jona-Lasinio model effective descriptions, *Eur. Phys. J. A* **57**, 234 (2021).
- [63] E. S. Fraga, L. F. Palhares, and T. E. Restrepo, Hot perturbative QCD in a very strong magnetic background, *Phys. Rev. D* **108**, 034026 (2023).
- [64] E. S. Fraga, L. F. Palhares, and T. E. Restrepo, Cold and dense perturbative QCD in a very strong magnetic background, *Phys. Rev. D* **109**, 054033 (2024).